Technical Paper

ISSN 1997-1400 Int. J. Pavement Res. Technol. 8(5):346-352

Seasonal Analysis of Flexible Pavement Response to Falling Weight Deflectometer

Mohammad Hossein Shafiee[1], Leila Hashemian[1], and Alireza Bayat[1+]

Abstract: Seasonal variation in pavement material properties can affect the in-situ measured pavement responses including deflections, stresses and strains. While previous field studies have mostly focused on the seasonal changes in Falling Weight Deflectometer (FWD)'s deflection basin, the simultaneous variations of stresses and strains were not usually monitored. The present study assesses seasonal impact on horizontal and vertical strains at the bottom of Hot Mix Asphalt (HMA) as well as unbound layers' stress at different depths. Several FWD tests were conducted from October, 2013 to December, 2014 in instrumented test road facility in Edmonton, Alberta, Canada. The obtained results showed that the pressure on top of base layer in the thaw season can exceed the one in the freeze season twice as much. Similarly, significant seasonal variations of horizontal and vertical strains at the bottom of the HMA were noticed. The present study concludes that using backcalculated layers' moduli may result in overestimation of the vertical stress within unbound layers and HMA horizontal strain, while underestimating HMA vertical strain.

DOI: 10.6135/ijprt.org.tw/2015.8(5).346

***Key words**: Backcalculation; Falling weight deflectometer; Pavement response; Seasonal variation.*

Introduction

Seasonal variation in material properties of flexible pavement may cause significant changes in pavement responses such as stress, strain and deflection within the structure. On the other hand, according to the Mechanistic Empirical Pavement Design Guide (MEPDG) [1], long-term pavement performance prediction models are considerably influenced by the critical pavement responses under loading. Therefore, it is crucial to evaluate the seasonal variation of pavement layers' characteristics via nondestructive testing equipment such as Falling Weight Deflectometer (FWD) [2]. Several researchers have attempted to theoretically investigate the seasonal changes in pavement responses based on the measured surface deflection basins under FWD and backcalculation of different pavement layers' moduli [3-5]. However, few field experiments have been conducted to investigate direct measurement of strain changes at the bottom of the Hot Mix Asphalt (HMA) and stress changes within unbound layers due to seasonal variations. Under the Seasonal Monitoring Program (SMP) of the Federal Highway Administration Long Term Pavement Performance (LTPP), seasonal change in the horizontal strain at the bottom of the HMA and vertical strain on top of the subgrade were modeled through layered elastic approach [3]. This research showed that thaw weakening of the structure can pose a concern in terms of greater vertical strain on top of the subgrade, whereas the summer's horizontal strain was critically high. In a study conducted by Simonsen et al. (1997), approximation of asphalt and subgrade strains using finite element modeling (FEM) revealed noticeably higher subgrade strains during the thaw period, while maximum asphalt strain occurred when surface temperature was the highest [4].

Based on several studies conducted at instrumented pavement sections to measure pavement response under FWD, a wide range of error exists between the measured and theoretically predicted values Ullitdz et al. (1994) [6] conducted FWD tests in southern Sweden and the Danish Road Testing Machine (RTM) to measure tensile strain at the bottom of the HMA and stress on top of the subgrade. Utilizing MODULUS 4.0 [7] to backcalculate the layer's moduli and using WES5 [8] computer program to predict responses, the study revealed discrepancy between the measured and the predicted values. This research indicated that non-linear elastic behavior of subgrade soil is probably attributed to disagreement between the measured and the predicted responses. Performing FWD tests along an instrumented pavement section in Oklahoma, Taylor et al. (2009) [9] also reported 104 to 164 and 4 to 22 percent prediction errors between measured and predicted stresses on top of the natural subgrade and the granular base, respectively. They concluded that invalid underlying assumptions in the linear elastic theory such as consideration of homogeneous, isotropic, and linear elastic materials and also static modeling of the FWD load rather than a dynamic impulse load are responsible for the observed discrepancies. In an attempt to predict horizontal strain in HMA and stress within unbound layers, simulation of FWD was performed using three-dimensional Finite Element Model (FEM) while considering subgrade as a nonlinear elastic layer [10]. This research showed that measured values were over-predicted from 20 to 49 percent on average irrespective of FWD loading magnitude. It was concluded that due to the temperature gradient across the thick HMA layer, consideration of one single backcalculated modulus for the whole layer can lead to erroneous predictions.

The scope of the aforementioned studies has not generally included a year-round series of FWD tests to validate the accuracy of using backcalculated layers' moduli for response prediction. However, the seasonal monitoring of stresses and strains can provide more insight in terms of both seasonal variation of

[1] University of Alberta, Markin/CNRL Natural Resources Engineering Facility, 9105 116th St., Edmonton, AB Canada T6G 2W2.

[+] Corresponding Author: E-mail bagdatbt@yahoo.com

Note: Submitted March 21, 2015; Revised September 9, 2015; Accepted September 11, 2015.

pavement material, as well as effectiveness of backcalculated layers' moduli for response prediction. The present study was conducted at Integrated Road Research Facility (IRRF)'s test road facility in Edmonton, Alberta, Canada to address the seasonal variation in pavement responses from October, 2013 to December, 2014. Horizontal and vertical strain at the bottom of the HMA, as well as vertical stress within unbound layers were monitored through several applications of FWD test on top of Asphalt Strain Gauges (ASG) and Earth Pressure Cells (EPC). In addition to seasonal monitoring of the induced responses, the accuracy of using backcalculated layers' moduli for prediction of the in-situ measured responses in different seasons was also evaluated.

Overview of IRRF Test Road Facility

The IRRF's test road facility is the new access road to Edmonton Waste Management Center (EWMC) located in the Northeast of the City of Edmonton, Alberta, Canada. Once opened to traffic, the test road is subjected to more than 500 garbage trucks per day, transporting waste materials to EWMC. The test road comprises two approximately 100-m apart pavement monitoring sections with 250-mm HMA layer, placed on top of a 450-mm granular base course (GBC) on top of clayey sand subgrade (SG) soil.

During construction in the summer of 2012, the test sections were instrumented with ASGs (Model CEA-06-125UT-350 from the CTL Group) and EPCs (Model LPTPC12-S from rst instruments) at different depths in the unbound layers. High-speed CR9000X datalogger from Campbell Scientific Corp Canada is used to collect the dynamic responses of both sections at 500 Hz under current FWD tests as well as future traffic. Both sections are similarly instrumented at the bottom of the HMA layer with six ASGs laid in the longitudinal direction (ASG-L), six ASGs laid in the transverse direction (ASG-T) and six vertical ASGs (ASG-V). Fig. 1(a) and (b) show the instrumentation layout, which is replicated in the two sections at the IRRF's test road. One array of ASG was laid along the outer wheelpath (OWP). To ensure repeatability and reliability of measurements under live traffic, the arrangement of the ASGs along the OWP was replicated in two additional lines, 600 mm to the right and 600 mm to the left of the OWP. EPCs were installed at two locations, on the OWP and on the inner wheelpath (IWP). As seen in Fig. 1(c), each location includes three EPCs installed at three different depths. EPC 1 and 2 were installed on the top of the GBC; EPC 3 and 4 were installed at the top of SG, and EPC 5 and 6 were installed at 1000-mm from the top of SG layer to monitor the distribution of load in the pavement underlayers.

Results and Discussion

FWD Testing Results in Different Seasons

FWD tests were conducted in October 2013 and April, July, September, October, November, December 2014 at specific sensor locations. During the testing, the HMA layer temperature was measured at 20 mm from the surface. At each test location, three drops were embarked at three stress levels using a Dynatest 8000 with sensor offsets at 0, 200, 300, 450, 600, 900, 1200 mm from the center of the load plate.

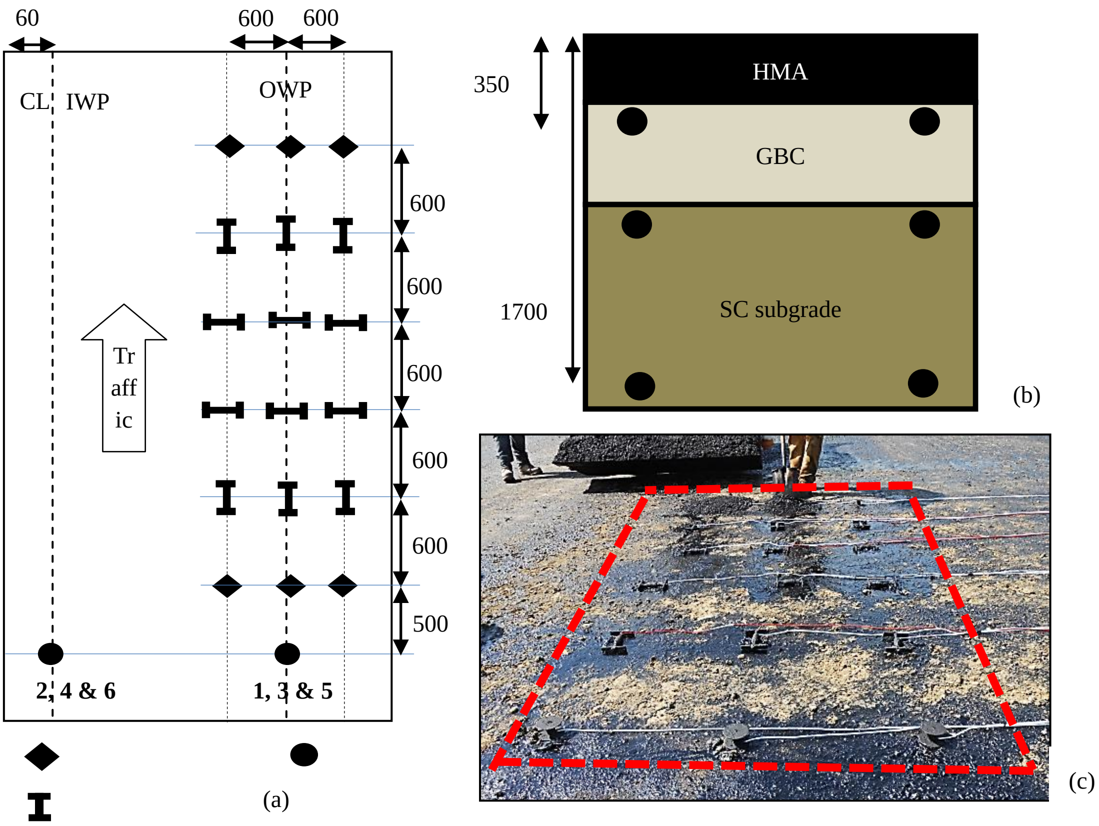

Fig. 1. (a) Schematic of Instrumentation (b) Schematic Cross Section and the EPC Locations (c) Installation of Sensors at the Bottom of the HMA (All Dimensions are in mm).

Three FWD drops were conducted at three locations along the OWP: on top of ASG-T 2, ASG-V 2 and EPC 1, 3 and 5. In each FWD test, a total of three pulses from each one of the sensors representing horizontal tensile strain (ε_t) , vertical compressive strain (ε_v) both at the bottom of the HMA, stress (σ_v) at top of the GBC and σ_v on top of SG and σ_v at 1000-mm within SG were available for analysis. It should be noted that the FWD tests conducted at one gage location resulted in negligible responses at adjacent gage locations, and thereby this study focuses only on the pulses under the load plate.

To compare deflection variations in different seasons, deflection basins obtained on top of EPC 1 were plotted for the seven FWD tests in Fig. 2. Comparison of deflection bowls evidently indicated lower deflections in colder months of the monitoring period and higher deflections during the thaw period. Results showed that the maximum central deflection under the load plate recorded in April, 2014 was 10 times larger than the minimum corresponding value in December, 2014. FWD tests performed in freeze period (i.e. November, 2014 and December, 2014) resulted in almost similar deflection basins. Also, consistent deflection basins were observed in October, 2013 and October, 2014 as the pavement was not subjected to traffic load over this time period.

Analysis of pavement instrumentation responses was conducted to monitor the seasonal variation of σ_v within unbound layers as well as the ε_t and ε_v at the bottom of the HMA. The distribution of σ_v within the base and subgrade can be investigated when the FWD loading was conducted over EPC 1 which is located on top of EPC 3 and EPC 5. The analyses of the σ_v measured by EPC 1, EPC 3 and EPC 5 were performed to investigate the impacts of depth and FWD stress levels on the σ_v. Fig. 3(a) shows the variation of σ_v measured on top of the GBC when subjecting the pavement to three FWD stress levels. The collected data suggests a consistent increase in the σ_v as the stress levels increased. Testing at the highest FWD stress, maximum recorded σ_v of 32.0 kPa occurred in April, 2014 and minimum value was determined to be 14.5 kPa in December, 2014 implying a noticeable decrease through evolution of recovery followed by freeze periods. Furthermore, the average increase in the σ_v at GBC was 54 and 123 percent when the average FWD stress increased from 386 to 566 and 762 kPa, respectively. Fig. 3(b) also depicts the changes in σ_v measured on top of SG showing that the recorded pressure ranged between 13.0 kPa (April, 2014) and 4.2 kPa (December, 2014) under the highest FWD stress level. The increasing trend of the measured σ_v versus higher FWD stress levels was observed, indicating on average 45 and 88 percent larger values when subjecting the pavement to drop 2 and 3, respectively. In an attempt to evaluate the decrease of σ_v in depth, it was found that σ_v on top of SG was 68 percent less than the associated value on top of GBC in December 2014, while the difference decreased to 28 percent in October 2014. Looking at variation of the σ_v at 1000-mm depth within SG as illustrated in Fig. 3(c), the proportion of the pressure resulting from uniformly distributed circular load of FWD load in SG was not significant. The range of variability of σ_v was from 5.0 to 0.7 kPa under the highest FWD stress level. Overall, the recorded σ_v at 1000-mm depth within SG showed 49 and 120 percent increase as the average FWD stress level increased by 47 and 98 percent, respectively. The ratios between the σ_v values recorded in April-2014 and December-2014 were 2.2 on top of the

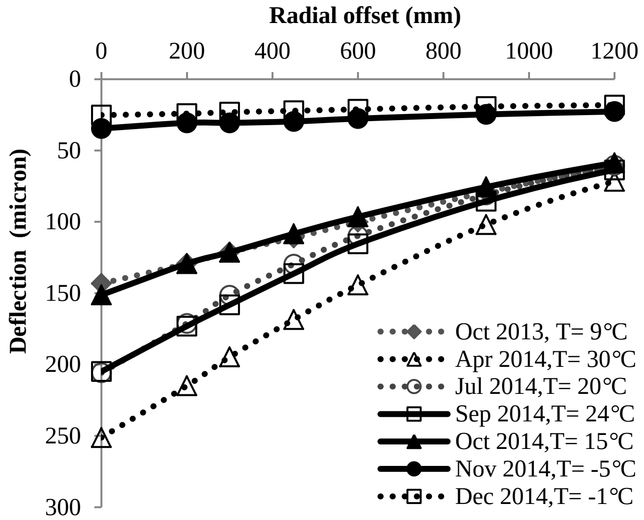

Fig. 2. Comparison of Deflection Basins for Different FWD Tests.

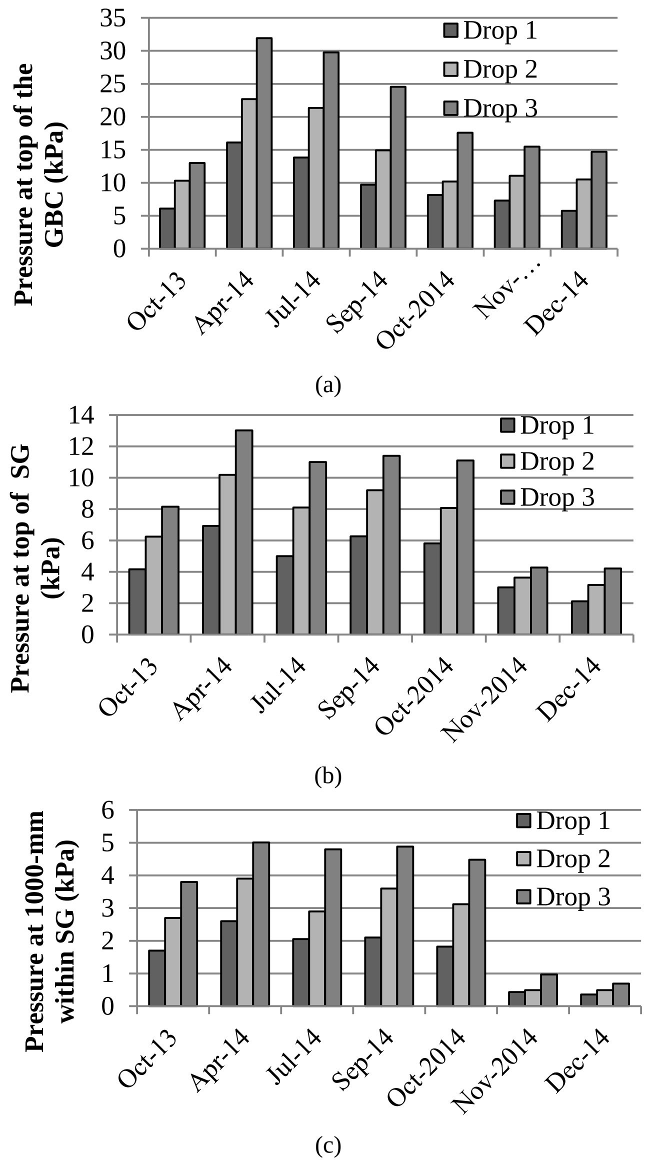

Fig. 3. Measured Vertical Stresses at (a) Top of the GBC, (b) Top of SG and (c) 1000-mm depth Within SG.

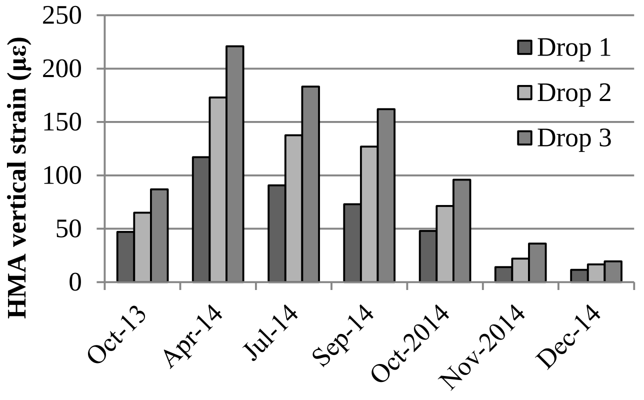

(a)

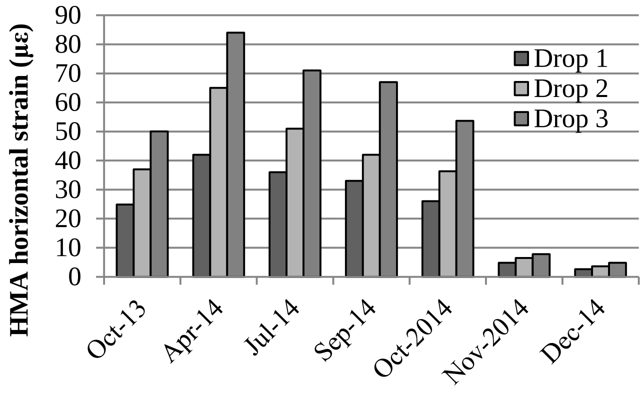

(b)

Fig. 4. Measured (a) Vertical Strain and (b) Horizontal Strain at the Bottom of HMA.

GBC, 3.1 on top of SG and 7.1 at 1000-mm within SG.

Strain measurements at the bottom of the HMA layer are provided in Fig. 4(a) and (b). Fig. 4(a) presents the ε_v at the bottom of the HMA layer under the three FWD stress levels for the test conducted at ASG-V2 location. As expected, the maximum ε_v of 221 microstrain occurred in April-2014 when pavement experienced the thaw period, whereas the minimum value of 19 microstrain was recorded in December-2014 as a result of freezing. The obtained difference between maximum and minimum observed ε_v confers a pronounced dependency of such response to seasonal variation. Besides, ε_v generally remained higher in April, July and September of 2014 signifying the importance of potential rutting in HMA at higher temperatures. In order to understand the stress-strain behavior of the HMA layer, the increments in ε_v were calculated as 52 and 106 percent when the FWD stress increased by 47 and 98 percent on average. Fig. 4(b) depicts the ε_t at the bottom of the HMA layer measured by ASG-T2 under three FWD load drops for the tests conducted directly over ASG-T2. Evaluation of ε_t ranging from a low of 5 micorstrain to a high of 84 microstrain revealed an identical behavior of response against seasonal change as explained for σ_v and ε_v previously. Although the magnitude of ε_v was approximately 2.3 times larger than those of ε_t for all the collected data, strong linear relationships were still evident for the FWD stress levels and ε_t. It means that ε_t exhibited 41 and 94 percent increase in parallel with 47 and 98 percent increase of stress exerted by FWD. According to Fig. 4(b), HMA layer was more prone to development of bottom-up fatigue cracking in April-2014 when it endured the maximum tensile strains. Based on Fig. 4, ε_v and ε_t measured in April-2014 were 11.3 and 17.3 times larger than the corresponding values measured in December-2014, respectively.

To investigate the probable source of variation in the responses obtained in different seasons, deflection history data collected for each FWD test was also analyzed. Knowing that the variation of pavement behavior across different seasons can also be evaluated using deflection time history data [11], the exerted FWD load attributed to the medium stress level was plotted against central geophone. As shown in Fig. 5, the largest hysteresis curve was captured in April-2014 when pavement structure was weak due to thawed unbound layers and asphalt temperature was the highest. Hence, as the pavement temperature increased, the hysteresis curves tended to reflect more viscoelastic behavior of HMA. According to Fig. 5, more plastic deflections were noticed in the warmer months which can be attributed to the viscous behavior of the HMA. This is in line with the higher magnitudes of ε_t and ε_v in the warmer months due to the lower stiffness of HMA. Hence, higher proportion of the applied FWD stress reaches to the unbound layer as previously shown in Fig. 3.

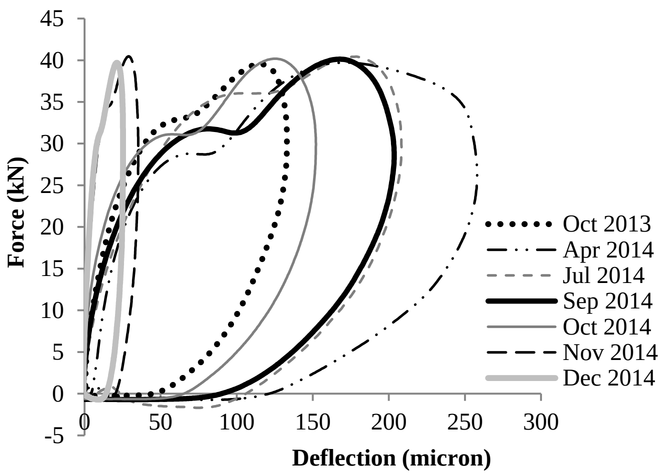

Fig. 5. Hysteresis Curves for Different FWD Tests.

Backcalculations of Layers' Moduli

To interpret the FWD deflection data, the peak values from each geophone's deflection time history were used to determine pavement layers' moduli through static backcalculation. The deflection basins recorded at the three test locations were used to determine the pavement layer's moduli. The deflection basins recorded at the three test locations had negligible differences, therefore the deflection basins obtained from the FWD tests conducted on top of EPC 1 were used for backcalculation. To investigate the agreement between the predictions and the measured pavement's structural responses, layers' moduli needed to be established first. To do so, deflection data from the FWD tests were used to backcalculate the pavement layers' moduli according to ASTM D5858 [12]. EVERCALC [13] was used to backcalculate the elastic modulus of the HMA (EHMA), GBC layer (EGBC) and SG layer (ESG). EVERCALC includes the WESLEA forward calculation subroutine to predict the pavement's structural responses and uses a modified Augmented Gauss-Newton algorithm for solution optimization. A stiff layer was considered in EVERCALC (the depth calculated internally), and the HMA modulus was set to be corrected internally based on the HMA temperature measured during testing.

In order to initialize the backcalculation process, each layer's seed modulus needs to be defined by the user. Due to its viscoelastic properties, EHMA strongly depends on the loading frequency and temperature. In order to define a proper seed value for EHMA, the laboratory-determined HMA mixture master curve was constructed based on AASHTO TP79 [14] as shown in Fig. 6(a) and (b). In order to find the appropriate loading frequency for the FWD tests, the average pulse duration measured by EPC 1, EPC 3 and EPC 5 was used according to Fig. 6(c). Results showed that the pulse duration did not vary amongst all FWD tests and also remained nearly constant at different depths below the surface. Thus, pulse duration determined by doubling the time elapsed from the beginning of the pulse to the peak in the first half of the pulse was calculated equal to 30 ms and selected as the representative pulse duration for further conversion to loading frequency. Therefore, EHMA values associated with 33 Hz loading frequency, calculated based on the inversed pulse duration, were derived according to the developed master curve as summarized in Table 1.

Typical values of 100 and 50 MPa recommended in ASTM D5858 were used to define the seed values for EGBC and ESC, respectively. Further, Poisson's ratio was defined as 0.35, 0.4 and 0.4 for HMA, GBC and SG soil, respectively, as outlined in ASTM D5858. Table 1 also shows the backcalculated layers' moduli in addition to the Root Mean Square Errors (RMSE) for individual FWD tests. It is worth noting that two percent limit recommended by ASTM D5858 was used as the criteria to select acceptable backcalculation results. It is noteworthy that backcalculation of layers' moduli for FWD tests performed in November and December of 2014 did not return acceptable RMSE values probably due to the frozen condition of the unbound layers and high stiffness of the HMA layer at subzero temperature; thereby, the two FWD tests were excluded for further analysis of the responses.

Analysis of Calculated Responses

To evaluate the validity of the backcalculated moduli, pavement responses were calculated using KENLAYER [15]. To pursue this purpose, the EVERCALC-backcalculated moduli were used to define each layer's properties in each FWD test when using KENLAYER. The loading was defined as static, uniform circular load, resulting in FWD stress levels. Note that the analysis focuses only on the responses under the center of the FWD load plate, since the induced responses at adjacent gage locations were negligible. To do so, the validated models were used to extract the pavement structural responses to the three FWD stresses at each gage location. Table 2 presents the KENLAYER-predicted responses and the errors in prediction of in-situ measured values for all FWD tests. Percent of Prediction Errors (*PPE*) defines the accuracy of theoretical values according to Eq. (1):

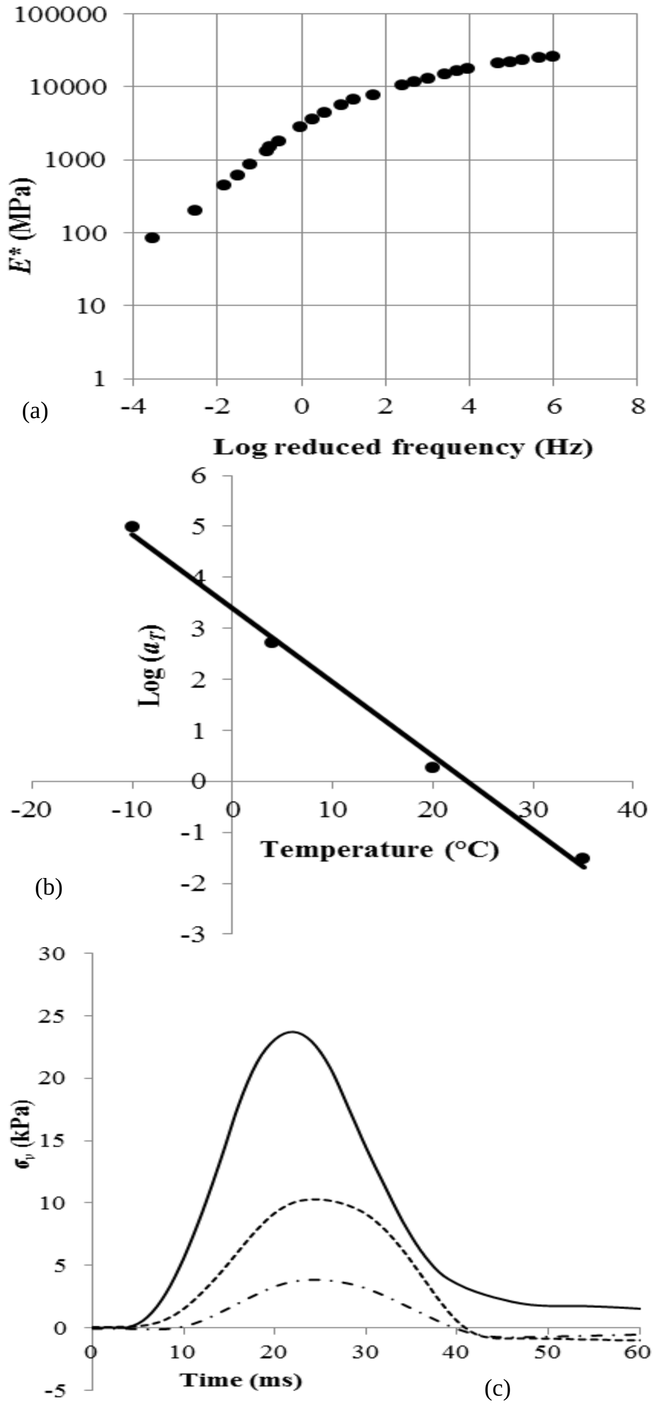

Fig. 6. (a) Master Curve and (b) Shift Factor for the HMA, (c) Typical Stress Pulses at Different Depths for Apr-2014 Test.

$$PPE = ((M - P)/P) \times 100 \tag{1}$$

where, *M* is the measured response and *P* is the predicted response.

According to Table 2, except for the ε_v at the bottom of HMA, other responses were overestimated when using backcalculated set of moduli in KENLAYER. It appears that the pattern of response variation with seasonal change in material properties was successfully captured through simulation of FWD tests. Taking the PPE of ε_t into account, the average PPE of the test in October, 2013

Table 1. Summary of Layers' Moduli from Laboratory and FWD-backcalculation.

Test	Temperature at 20-mm Depth (°C)	Laboratory	Backcalculation			*RMSE*
		E_{HMA} (MPa)	E_{HMA} (MPa)	E_{GBC} (MPa)	E_{SG} (MPa)	(Percent)
Oct-13	9	15640	10650	188	152	1.76
Apr-14	30	4100	2980	170	107	0.46
Jul-14	20	8500	3410	296	112	0.59
Sep-14	24	6300	4325	212	106	0.47
Oct-14	15	12340	9115	210	149	0.50

Table 2. Summary of Predicted Responses and Prediction Errors.

Test	FWD Stress (kPa)	σ_v at GBC		σ_v at SG		σ_v at 1000-mm Within SG		ε_v at the Bottom of HMA		ε_t at the Bottom of HMA	
		P [a] (kPa)	*PPE* (Percent)	*P* (kPa)	*PPE* (Percent)	*P* (kPa)	*PPE* (Percent)	*P* (με)	*PPE* (Percent)	*P* (με)	*PPE* (Percent)
Oct-13	391	12.0	-49	6.8	-39	2.8	-40	34	39	30	-18
	565	17.4	-41	10.0	-38			50	30	45	-17
	732	23.3	-44	13.5	-39			67	30	60	-17
Apr-14	380	21.6	-25	9.8	-29	3.3	-21	84	8	91	-54
	561	31.9	-29	14.4	-30	4.9	-20	125	8	134	-52
	744	42.7	-25	19.3	-33	6.5	-23	167	3	180	-53
Jul-14	379	21.3	-35	9.4	-47	3.2	-36	4.1	-35	66	-45
	572	31.4	-32	13.9	-42	4.7	-39	5.6	-32	97	-47
	758	42.1	-29	18.6	-41	6.3	-24	155	18	129	-45
Sep-14	382	18.0	-23	10.5	-44	3.2	-28	69	7	59	-44
	569	26.5	-11	15.4	-44	4.7	-20	101	26	87	-52
	764	35.5	-8	20.6	-47	6.3	-23	135	20	117	-43
Oct-14	381	13.4	-39	8.2	-29	2.8	-36	38	26	34	-23
	566	20.0	-49	12.2	-34	4.2	-26	56	26	50	-28
	761	26.8	-34	16.4	-32	5.7	-21	75	28	76	-29

[a] Predicted value

was -17 and it remained almost consistent in October, 2014 equal to -26. However, the average PPE decreased to -53, -45 and -46 in April, July and September of 2014, respectively. This shows higher discrepancies between measurement and prediction in thaw and summer periods. The absolute average PPE values of 32 for σ_v at top of GBC, 38 for σ_v at top of SG and 28 for σ_v at 1000-mm depth within SG are reasonably comparable with the average error of 30 percent reported by Yin (2012) [10] through 3-D finite element modeling of flexible pavement response to FWD in Blair County, Pennsylvania. In addition, averaged PPE values of the σ_v at three depths were determined equal to -35 percent for drop 1, -32 percent for drop 2 and -30 percent for drop 3 suggesting the independence of PPE on FWD stress.

Fig. 7 illustrates the variation of PPE against different response types. The PPE associated with σ_v at top of GBC varied in a larger range of values than other responses. For σ_v recorded at top of SG, the median of PPE values was the lowest, while the PPEs were more in agreement with each other in comparison to the cases of σ_v recorded at top of GBC and at 1000-mm within SG. Furthermore, PPE values for ε_v had a better level of agreement with each other when compared to those of ε_t. Using the linear elastic approach, average PPE for ε_t was determined to be -37, while it was near 20 for ε_v.

This analysis shows that consideration of linear elastic isotropic and homogenous materials, and static circular loading of FWD can contribute to inaccurate backcalculation of layers' moduli and consequently erroneous prediction of response. To summarize, direct validation of theoretically calculated responses in the field and their comparison to the in-situ measured responses revealed the potential error in application of commonly-used FWD analysis methods.

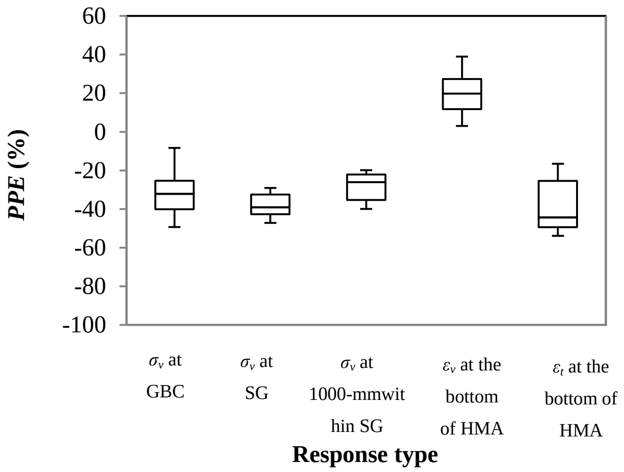

Fig. 7. Comparison of Response Prediction Errors.

Conclusions

FWD tests were performed directly on top of ASGs and EPCs embedded in the IRRF test road in Edmonton, AB, Canada, to monitor the seasonal variation in pavement responses. This paper focused on the evaluation of horizontal (ε_t) and vertical (ε_v) strains at the bottom of the HMA layer, as well as the vertical pressure (σ_v) at different depths within the unbound layers when subjected to FWD testing. The maximum values of recorded strains and stresses occurred in April, 2014 due to thawing in pavement layers. As a result, σ_v on top of the GBC recorded in the thaw season was 2.2 times larger than the corresponding values in the freeze season. Besides, ε_v and ε_t at the bottom of the HMA layer were also 11.3 and 17.3 times larger than those in Dec-2014, respectively. Using hysteresis curves for each test, it was found that higher measured responses in warmer months can be attributed to the more viscous behavior of the HMA. Comparisons were made between the in-situ measured and predicted responses using EVERCALC-backcalculated-layers' moduli in KENLAYER. It was observed that using a computer simulation led to over-prediction of σ_v within unbound layers and εt at the bottom of the HMA, while ε_v values at the bottom of the HMA were generally underestimated. The average Percent of Prediction Error (PPE) values were found equal to -32 for σ_v on top of the GBC, -38 for σ_v on top of SG, -28 for σ_v at 1000-mm within SG, 20 for ε_v at the bottom of the HMA and -37 for ε_t at the bottom of the HMA. It was found that the magnitudes of PPEs associated with σ_v at GBC varied in a larger range when compared to other responses. However, a better level of agreement was observed between PPEs of ε_v rather than those of ε_t both at the bottom of the HMA. Finally, the average PPEs tended to be higher during warmer months due to the deviation of HMA behavior from linear elasticity.

Acknowledgements

The authors would like to acknowledge Alberta Transportation, Alberta recycling, and The City of Edmonton for providing financial and in-kind support for the construction and instrumentation of the IRRF's test road. Alberta Transportation is also acknowledged for conducting the falling weight deflectometer (FWD) tests for this study. The close cooperation of Tetra Tech EBA FWD test crews during testing is also greatly appreciated.

References

1. ARA, Inc. (2004). ERES Consultant Division. Guide for Mechanistic–Empirical Design of New and Rehabilitated Pavement Structures. Final report, *NCHRP Project 1-37A*. Transportation Research Board of the National Academies, Washington, DC, USA. http://www.trb.org/mepdg/guide.htm.
2. Shahin, M.Y. (2005). *Pavement management for airports, roads, and parking lots*, Springer Science & Business Media, Inc., New York, NY, USA.
3. Drumm, E.C. and Meier, R. (2003). LTPP data analysis: daily and seasonal variations in in situ material properties, Transportation Research Board, National Research Council, Washington, DC, USA.
4. Simonsen, E., Janoo, V.C., and Isacsson, U. (1997). Prediction of pavement response during freezing and thawing using finite element approach, *Journal of Cold Regions Engineering*, 11(4), pp. 308-324.
5. van Gurp, C. (1995). Characterization of seasonal influences on asphalt pavements with the use of falling weight deflectometers. TU Delft, Delft University of Technology, Delft, The Netherlands.
6. Ullidtz, P., Krarup, J., and Wahlman, T. (1994). Verification of Pavement Response Models. Nondestructive Testing of Pavements and Backcalculation of Moduli, *ASTM STP 1198*, A.J. Bush, G.Y. Baladi, Eds., pp. 143-158.
7. Scullion, T., Michalak, C.H. (1991). MODULUS 4.0, User's Manual. Texas Transportation Institute, Research Report 1123-4, The Texas A&M University System, College station, TX, USA.
8. Van Cauwelaert, F.J., Alexander, D.R., White, T.D., and Barker, W.R. (1989). Multilayer Elastic Program for Backcalculating Layer Moduli in Pavement Evaluation. Nondestructive Testing of Pavements and Backcalculation of Moduli, *ASTM STP 1026*, A.J. Bush, G.Y. Baladi, Eds., pp. 171-188.
9. Taylor, P., Solanki, P., Zaman, M., Muraleetharan, K.K., and Timm, D. (2009). Evaluation of Resilient Moduli of Pavement Layers at an Instrumented Section on I-35 in Oklahoma, *Road Materials and Pavement Design*, 10(1), pp. 167-188.
10. Yin, H. (2012). Simulation of Flexible Pavement Response to FWD loads: A mechanistic Approach, *International Journal of Pavement Research and Technology*, 5(4), pp. 257-266.
11. Deblois, K., Bilodeau, J.P., and Dore, G. (2010). Use of falling weight deflectometer time history data for the analysis of seasonal variation in pavement response. *Canadian Journal of Civil Engineering*, 37(9), pp. 1224-1231.
12. ASTM (2008). Standard Guide for Calculating In Situ Equivalent Elastic Moduli of Pavement Materials Using Layered Elastic Theory. ASTM D 5858-96, West Conshohocken, PA, USA.
13. Mahoney, J.P., Coetzee, N.F., Stubstad, R.N., and Lee, S.W. (1989). A performance comparison of selected backcalculation computer programs. Nondestructive Testing of pavements and Backcalcation of Moduli, *ASTM TP 1026*, A.J. Bush, G.Y. Baladi, Eds., pp. 452–467.
14. AASHTO (2009). Determining the Dynamic Modulus and Flow Number for Hot Mix Asphalt (HMA) Using the Asphalt Mixture Performance Tester (AMPT), AASHTO TP79-09, American Association of State Highway and Transportation Official, Washington, DC, USA.
15. Huang, Y.H. (1993). *Pavement analysis and design*. 2nd Edition, Prentice Hall, Inc., Upper Saddle River, NJ, USA.